THE ONSET OF AMYLOID BETA PEPTIDE AGGREGATION

Alexandra Seuthe
ARC/UC LEADS, Biochemistry

ABSTRACT

A potentially important aspect of Alzheimer's disease is believed to be amyloid beta (Aß) peptide aggregates that form plaques in the brain. This study focuses on the initial stages of aggregation in the gas-phase, which are believed to be crucial to the formation of fibrils. The peptide we have studied is a 13 residue Aß peptide that is similar to amyloid fragments studied in solution that exhibit fibril formation. Electrospray Ionization (ESI) is used to form gas-phase peptide ions, and ion mobility techniques are used to analyze their conformation. The mass spectrum of the peptide yields mass-to-charge ratio values (m/z). Selection of a single m/z value will allow us to measure arrival time distributions (ATDs), obtain the ion mobility, and from the mobility, the cross section of the peptide ion. A theoretical fit to the experimental data will yield rate constants, and measuring these as a function of temperature will yield an energy barrier for dissociation of the cluster. Cross section measurements will be compared with molecular modeling calculations. As of the time of this publication, ESI has not been successfully used to analyze the Aß peptide. The use of this technique will be discussed for the peptides LHRH and bradykinin. Molecular modeling for the Aß peptide monomer and dimer, and conformational changes that occur with aggregation and dissociation will also be examined. These experimental and theoretical results will help us to better understand the noncovalent interactions between aggregates of small amyloid beta peptides. The ultimate goal of understanding the aggregation process is to learn how to manipulate this process. This might have significant medical applications to the treatment of Alzheimer's disease.

BACKGROUND

FIGURE 1

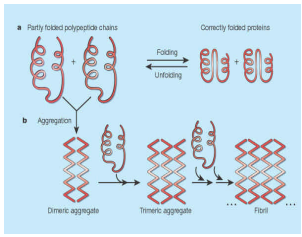

Figure 1: Aggregate formation during protein folding. The function of proteins is directly related to their shape because surface features of the protein create binding sites that are highly specific. **a.** During normal protein folding, polypeptide chains collapse into correctly folded, functional proteins. **b.** Errors in folding can occur when the hydrophobic side chains of partially folded proteins are exposed to the aqueous environment. These hydrophobic regions bind to similar surfaces on neighboring proteins in order to shield themselves from the aqueous environment. As the proteins bind, dimers, trimers, and high order clusters form.

FIGURE 2

PET Brain Scan

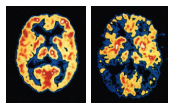

Normal Alzheimer's

Figure 2: Effect of Ab plaques in the brain. It has been suggested that Aβ peptide aggregates, which form plaques in the brain cause the neuronal degeneration and dementia that occur during Alzheimer's disease.

FIGURE 3

Ab Aggregation

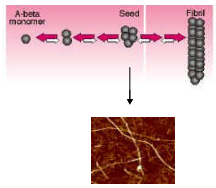

Fibril

Figure 4: Ab Aggregation. Aβ peptides aggregate to form fibrils. During this process, monomer peptide units aggregate into dimers, then trimers, and so on, until a fibril is formed.

FIGURE 4

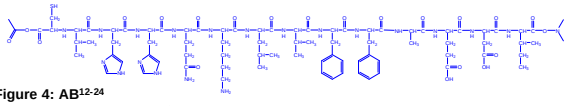

Figure 4: AB$^{12-24}$
13-residue fragment of the Aβ peptide. This peptide was chosen for study because it is one of the smallest Aβ peptides to exhibit aggregation.

EXPERIMENTAL TECHNIQUE

FIGURE 5

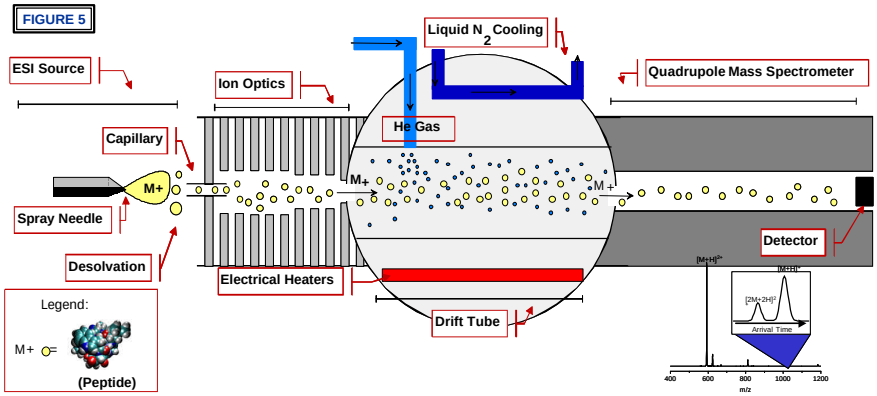

Figure 5: Schematic of the Electrospray Ionization Mass Spectrometer (ESI-MS).
Mass spectrometry has become an important tool to examine the conformations of proteins in the gas phase. This is not only due to advances in instrumentation, but also to the growing number of examples of non-covalent interactions that have found to be maintained in the gas phase. In our ESI technique, charged gas phase molecules are pulse-injected into a temperature and pressure regulated drift cell. The pulse of ions drifts through a helium buffer gas under the influence of a weak electric field. Upon exiting the cell, the ions pass through a quadrupole mass spectrometer to a detector where an arrival time distribution (ATD) of the mass-selected ion is collected.

FIGURE 6

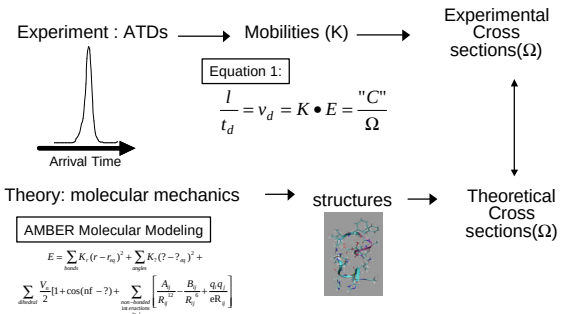

Figure 6:
a) The ion's arrival time is inversely proportional to its mobility and directly proportional to its cross section. Compact ions with smaller cross sections drift through the cell faster and have shorter arrival times. From the ATDs, the mobility of the ion can be obtained using Equation 1. From the mobility we can then calculate cross section.
b) To obtain conformation details about the ions measured in ion mobility experiments, cross sections extracted from ATDs are compared to calculated cross sections of theoretical models. The AMBER suite of MM/MD programs is used to provide theoretical structures.

FIGURE 7

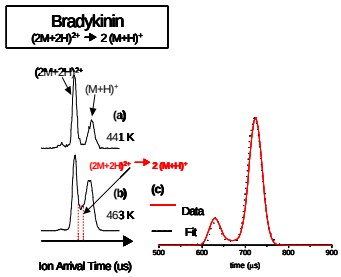

Figure 7 Theoretical fit for the ATDs of bradykinin.
a) At 441K, no dissociation occurs and the monomer and dimer peaks are baseline resolved. **b)** At 463 K, dissociation occurs, causing an intermediate arrival time to be measured. The indicated area represents the dimer molecules which are dissociating. **c)** A theoretical fit to the experimental data will yield the rate constant for the dissociation reaction at that temperature.

RESULTS AND DISCUSSION

FIGURE 8

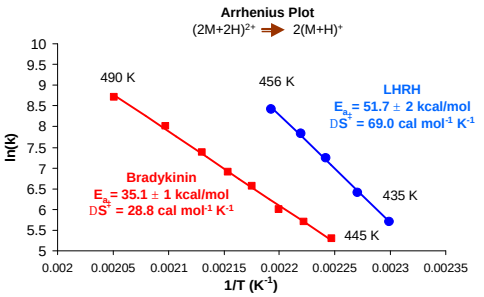

Figure 8 Arrhenius Plot for LHRH and Bradykinin.
The activation energies (E_a) and entropy (? S‡) values of the dimer dissociation reaction for LHRH (Luteinizing Hormone Releasing Hormone) and bradykinin have been successfully obtained by plotting the rate constant as a function of temperature. The slope of this line yields E_a and the intercept gives ? S‡.

FIGURE 9

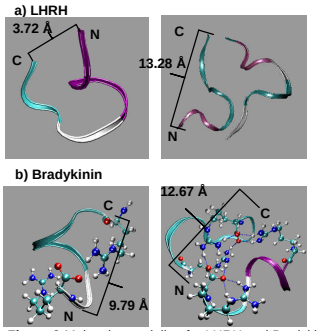

Figure 9 Molecular modeling for LHRH and Bradykinin.
Molecular modeling for the monomer and dimer of both peptides explains why LHRH has a higher E_a and ? S‡.
a) The LHRH monomer rearranges and opens up its backbone in order to associate with another monomer unit.
b) Bradykinin does not have to undergo as vast
Of a conformational change as LHRH.

FIGURE 10

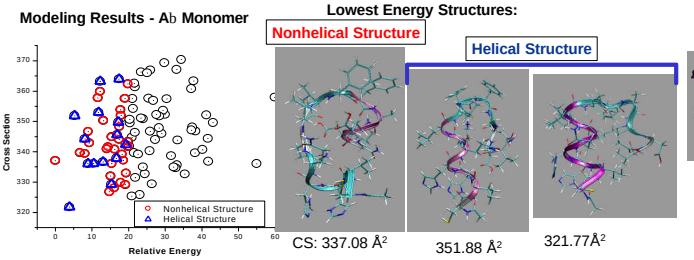

Figure 10: Modeling results for the Ab Monomer.

Modeling suggests that two structure types are possible for Aß12-24. The first type is U-shaped and contains very little helix. The second type is more linear and contains an extended helix at the N-terminus. These types will be designated as nonhelical, and helical. The nonhelical structure is predominant, accounting for 32 of the 44 structures in the lowest 20 kcal/mol.

The helical structure is more soluble than the nonhelical structure. This is due to the fact that helices are soluble because the hydrophobic regions of the peptide are buried in the core of the helix, allowing the hydrophilic regions to interact with the aqueous environment. The fact that two structures are found in modeling, one soluble and one insoluble suggests that during the aggregation process an intermediate Aß peptide exists, which is still soluble. A pathway then must exist by which the soluble Aß is able to polymerize into its fibrillar, insoluble form. Ion mobility studies of this peptide will be necessary to determine if we do see these two types of structures experimentally. Further modeling may suggest the mechanism by which these two peptides interconvert.

FIGURE 11

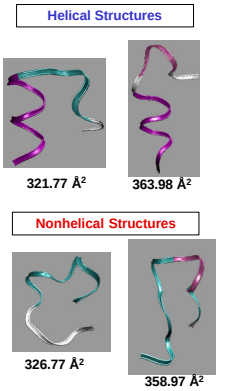

Figure 11: Ab Monomer Structures
Helical and nonhelical structures for the Aβ monomer occur at a range of cross sections. The nonhelical structure can occur at lower cross sections because it can compress and expand by varying the distance between its two termini. The helical structures can also compress and expand by varying the length of the helix.

FIGURE 12

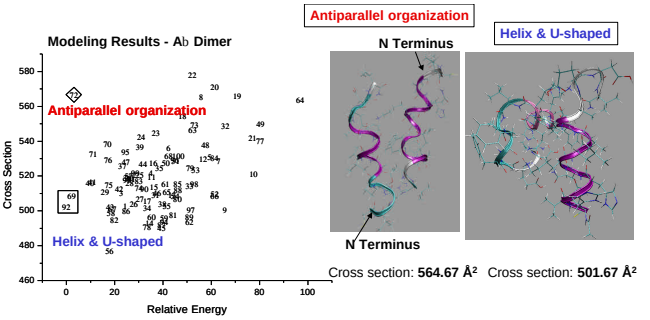

Figure 12: Modeling results for the Ab dimer.
Modeling suggests two types of structures, one which contains an anti-parallel association of two helix monomers, and one which contains a helix monomer associated with a U-shaped monomer. The dimer which contains two helices indicates that during the dimerization process the U-shaped monomer is able to rearrange its backbone to form a helix. This great conformation change will likely give high E_a and ? S‡ values, such as in the case of LHRH.
These calculations were carried out using the nonhelical structure as the initial structure. This structure was chosen because it was dominant in the lowest 20 kcal/mol of the calculated monomer structures.

FIGURE 13

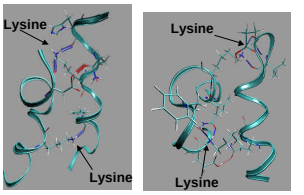

Figure 13: H-bond analysis of dimer.
In order to understand the interactions of the dimer aggregation, we performed a hydrogen bond analysis on the dimer. Hydrogen bonds with angles of less than 20 degrees, and distances of less than 3.3 A were detected. Analysis shows that lysine is heavily involved in aggregation, due to the protonated nitrogen on its side chain. In both low energy structures, the lysine in each monomer unit forms a hydrogen bond with the other monomer. This interaction contributes to the stability of the dimer, since the charged lysine stabilizes the large dipole moment of the dimer.

CONCLUSION

The instrumental technique outlined has been successful in studying the aggregation of LHRH and bradykinin. In the future, we will apply this technique to Aß peptides. Molecular modeling of the Aß12-24 monomer suggests that there are two possible conformations. Dimer calculations also show two possible structures, one which exhibits the antiparallel orientation found in beta sheets.

The study of Aß peptide aggregation is crucial because of its possible role in Alzheimer's disease. Studying the onset of aggregation is useful because it allows us to understand the aggregation process at a truly molecular level. If the mechanism of aggregation can be understood, then compounds can be developed in order to manipulate it.

ACKNOWLEDMENTS

This research would not have been possible without the guidance of my mentor Professor Michael Bowers, and the support of the ARC Program.
I would also like to thank Dr. Thomas Wyttenbach, Dr. Jennifer Gidden, Summer Bernstein, Erin Shammel, Catie Carpenter, and Professor Hugh Marsh.